J Appl Electrochem (2013) 43:839–846
DOI 10.1007/s10800-013-0571-0

ORIGINAL PAPER

Electrodeposition of Zn–SiC nanocomposite coatings

Gabriella Roventi · Tiziano Bellezze · Romeo Fratesi

Received: 19 March 2013 / Accepted: 4 June 2013 / Published online: 18 June 2013

Abstract Zn–SiC composite coatings were obtained on mild steel substrate by electrodeposition technique with high-current efficiency. A slightly acidic chloride bath, containing SiC nanoparticles and gelatine as additive, was used. The electrodeposition was carried out under galvanostatic control with pulsed direct current; the effect of experimental parameters (temperature, average current density and particles concentration) on composition, morphology and structure of the deposit was studied. Coatings were characterized by means of scanning electron microscopy, energy dispersive X-ray analysis, X-ray diffractometry and Vickers microhardness measurements. Zn–SiC electrodeposits with the best characteristics were obtained by performing electrodepositions at 45 °C, with 20 g L^{-1} SiC in the bath and with average current density in the range 100–150 mA cm^{-2}. Under these experimental conditions, homogeneous and compact coatings, with low-grain size and SiC content ranging from 1.7 to 2.1 wt%, were found to be electrodeposited. Microhardness measurements showed for these deposits an increase of about 50 % with respect to those without nanoparticles obtained in the same experimental conditions.

Keywords Composite coating · Zinc · SiC · Nanoparticles · Electrodeposition · Microhardness

1 Introduction

In the last few decades, the electrodeposition of composite coatings, formed by a metallic matrix containing ceramic micro or nanoparticles, has been the object of several investigations [1, 2]. The incorporation of ceramic particles leads to an improvement of mechanical [3], tribological [4] and corrosion [5] properties of the metallic coatings. Electrodeposition is a technique widely utilized to obtain metal matrix composites, due to its ease of use, low cost and versatility, compared to other preparation techniques [6]. Besides plating, the electrochemical production of composites can be used for new application fields, as electrocatalysis, photoactive materials and energy storage [1].

Exhaustive reviews of the significant literature have been published [1, 2, 7–9]. However, even though much research on inert particles incorporation in the electrodeposits has been carried out, the mechanism of this process is not yet well understood. Several theories have been proposed, including electrophoresis, mechanical entrapment, adsorption and convective-diffusion [2]. The first model, based on a two-step absorption mechanism of the particles, has been developed by Guglielmi [10]. Currently, the models used to describe inclusion of the particles are restricted to specific conditions, therefore, experimental tests remain very important [2].

Electrodeposited composite characteristics are influenced by deposition parameters, like current profile, bath composition, pH, particle concentration, presence of additives, temperature and bath agitation [2, 6, 11]. Furthermore, there is an important relationship between particle type, size and its incorporation rate [12, 13]. Between electrodeposit characteristics, the incorporated particle content is the most important, since it largely determines the composite properties, such as wear resistance and corrosion protection [6]. On the basis of literature, operating parameters which enhance the incorporation of inert particles in the deposit are: high-particles concentration in

G. Roventi (✉) · T. Bellezze · R. Fratesi
Department of Materials, Environmental Sciences and Urban Planning, Polytechnic University of Marche,
v. Brecce Bianche, 60131 Ancona, Italy
e-mail: g.roventi@univpm.it

the bath, low concentration of the electroactive species, smaller sized particles and pulsed current [2]. Furthermore, the use of ultrasound during electrodeposition reduces agglomeration and leads to a more uniform distribution of the particles, with a significant improvement in microhardness and wear resistance of the composite coating [14].

The metals mostly used as matrix are copper and nickel [2]; in particular Ni–SiC is the most studied system, due to its possible technological applications [2, 15].

Zinc-based coatings are widely used for sacrificial protection of steel, due to their low cost, high corrosion resistance and low environmental impact. On the other hand, zinc has low hardness and abrasion resistance, which can be improved by ceramic particle incorporation.

Electrodeposition of several zinc and zinc alloy composite coatings has been investigated. Tulio and co-workers [16, 17] studied the deposition of Zn, Zn–Co and Zn–Ni in presence of SiC or Al_2O_3 microparticles from sulphate baths. Müller et al. [18] studied the codeposition of α-SiC (ϕ 7 μm) with Zn–Ni alloy in alkaline solution. Zheng et al. [19] codeposited Al_2O_3 and Zn–Ni alloy from chloride bath and found an increase in corrosion resistance. Zn–TiO_2 composite electrodeposition has been studied from chloride bath [13], due to the semiconducting properties of TiO_2 with applications as photocatalysis, particularly, in the treatment of polluted water. Zn–ZrO_2 [20] and Zn–SiO_2 [21] nanocomposites have been successfully electrodeposited from sulphate baths.

The aim of the present work was to investigate the electrolytic codeposition of SiC nanosized particles with zinc on mild steel. A slightly acidic chloride bath widely utilized by galvanic industry for barrel process was used. The electrodeposition tests were performed with pulsed direct current. The effect of the experimental parameters on SiC incorporation rate, current efficiency, zinc preferential orientations, coating morphology and microhardness was studied.

2 Experimental

Pure zinc coatings were electrodeposited on mild steel substrate from a slightly acidic chloride bath, with the following composition: 70 g L^{-1} $ZnCl_2$, 185 g L^{-1} KCl, 26 g L^{-1} H_3BO_3 and 2 g L^{-1} gelatine (pH 5.7). On adding to the deposition bath 10 or 20 g L^{-1} SiC particles (Cometox^{TM} SiC 99 %, average crystallite size: 60 nm), Zn–SiC composite coatings were electrodeposited. All the solutions were prepared with analytical grade reagents and double distilled water.

The 'as received' SiC nanoparticles are agglomerated, as shown by their SEM image (Fig. 1); to disaggregate and to well disperse the particles, bath was stirred magnetically at room temperature for at least 24 h before the start of the

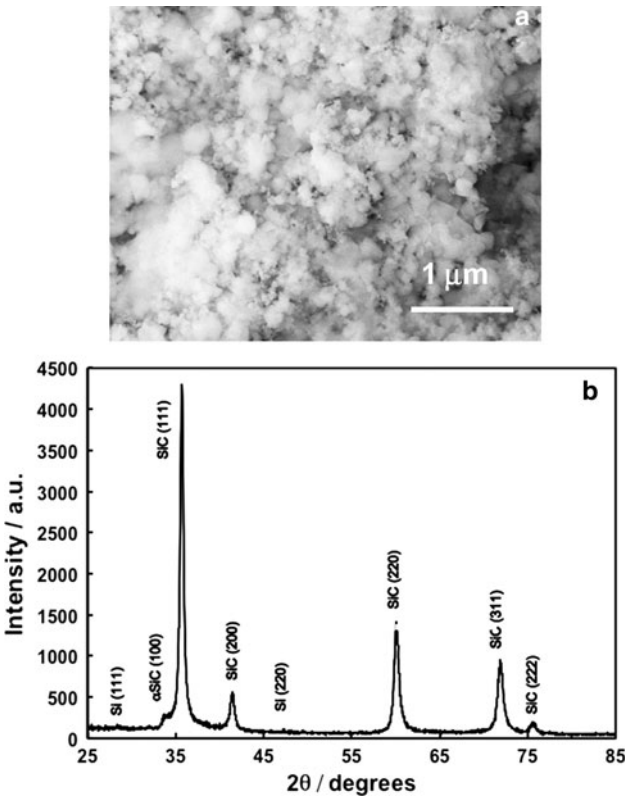

Fig. 1 **a** SEM image and **b** XRD pattern of the as received SiC nanoparticles

electrodepositions. Figure 1 shows also the X-ray diffractogram of the 'as received' particles: the 2θ angles of all the peaks well match with those of βSiC (JCPDS 29-1129, cubic structure), with the exception of the peak at 33.7°, related to the reflection from (100) planes of αSi (JCPDS 29-1130, hexagonal structure), and the two small peaks at 28.4° and 47.2°, related to (111) and (220) reflections, respectively, of Si (JCPDS 5-565).

Zeta potential measurements indicated that, in the chloride bath containing gelatine, SiC particles have a mean value of 0.5 ± 0.1 mV, as expected for particles having no net charge.

Electrodepositions were carried out at constant temperature (33 ± 1 or 45 ± 1 °C) under constant magnetic stirring (about 250 rpm). In fact, agitation affects particles incorporation process: high agitation generally increases the amount of particles in the deposit, but excessive agitation may lead to a decrease in particle incorporation rate because of the turbulent flow, which washes away nanoparticles from the cathode surface [6]. A 0.5-L glass beaker was used as electrochemical cell. The cathode was a mild steel disc, 1-mm thick, mounted in a flat specimen holder leaving an exposed area of 3.14 cm^2. Before the electrodepositions, the steel disk was mechanically polished with abrasive papers with different grades (320, 500 and 800 grit) degreased with acetone, rinsed with double

distilled water and dried. To reinstate Zn^{2+} ions reduced at the cathode, a 99 % zinc sheet (area 21 cm^2, thickness 0.1 cm) was used as anode. The cathode and anode were kept parallel at a distance of 4 cm. The reference was an Ag/AgCl electrode (207 mV vs. NHE), to which all the potentials are referred. After the electrodeposition tests, the cathode was removed from the cell, rinsed with distilled water and then immersed in an ultrasonic bath for 10 min, to remove SiC particles loosely adsorbed on the deposit surface; afterwards, the cathode was rinsed and dried.

The mass of the deposit was evaluated by weighing the mild steel disk before and after the electrodeposition. Coatings were analysed for Zn and Si by means of energy dispersive X-ray analysis (EDX) (Fig. 2); from the obtained percentages of Zn and Si (wt%), SiC wt% in the coating was calculated by means of the following formula:

$$\mathrm{SiC(wt\%)} = \frac{\mathrm{Si(wt\%)} + \frac{\mathrm{Si(wt\%)}}{\mathrm{PA_{Si}}}\mathrm{PA_C}}{\mathrm{Zn(wt\%)} + \mathrm{Si(wt\%)} + \frac{\mathrm{Si(wt\%)}}{\mathrm{PA_{Si}}}\mathrm{PA_C}} 100 \quad (1)$$

where PA_{Si} and PA_C are, respectively, Si and C atomic weights.

Zn partial current density was calculated from the weight of deposited Zn by means of the following equation, derived from Faraday's law [22]:

$$i_{Zn} = \frac{P_{Zn}F}{PE_{Zn}tA} \quad (2)$$

where i_{Zn} is Zn partial current density (mA cm^{-2}); P_{Zn} is the weight of deposited zinc (mg); F is the Faraday constant (96485 C); PE_{Zn} is Zn equivalent weight, t is the deposition time (s); and A is the working electrode area (cm^2). Hydrogen partial current density (i_{H2}) was calculated as the difference between total current imposed and i_{Zn}; current efficiency (η) was calculated as percentage of i_{Zn} with respect to the total current density.

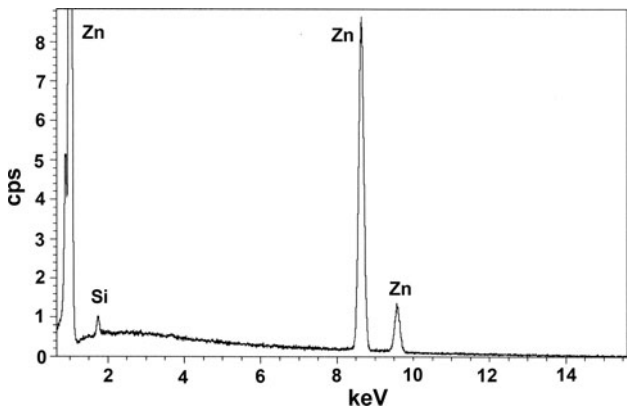

Fig. 2 EDX spectra of Zn–SiC coating (SiC_d 2.1 wt%) electrodeposited on mild steel. SiC_b 20 g L^{-1}; gelatine 2 g L^{-1}; 45 °C; average pulsed current density 150 mA cm^{-2}

Electrodepositions were carried out under galvanostatic control with pulsed direct current, using a cathodic square wave (pulse frequency 1 Hz, duty cycle 50 %); some preliminary tests were performed with direct current. For the experiments with direct current, an EG&G Princeton Applied Research Model 273 potentiostat was used. Electrodepositions with pulsed current were carried out by means of an Amel Model 2049 potentiostat and an Amel Model 568 function generator. Electrodeposition time was changed depending on current density in order to obtain coatings about 10 μm thick, except for the deposits to be submitted to microhardness measurements, for which deposition was prolonged until the thickness was 30 μm, to avoid the signal of the steel substrate.

All the tests were repeated three times.

The preferred crystallite orientations of the obtained Zn and Zn–SiC coatings were studied by means of X-ray diffraction analysis (XRD), by using a Philips PW 1730 diffractometer with Cu Kα radiation ($\lambda = 0.154$ nm). Morphology and chemical composition of the coatings were studied by scanning electron microscopy (SEM) coupled with EDX. A Zeiss Supra 40 microscope and a Bruker Quantax serie 5000 L N_2-free XFlash device were used.

Zeta potential of SiC particles in the deposition bath was measured at 25 °C by means of a Malvern Nano-ZS apparatus.

Vickers microhardness tests were performed on deposit surface by applying a 10 g load for 10 s. A HX-1000 Remet equipment was used.

3 Results and discussion

Preliminary tests were performed in order to select the additives for the plating bath and their concentration. In fact, nanoparticles agglomerate very easily in the plating bath because of their high-surface area; this phenomenon corresponds to a greater amount of agglomerated particles in the deposit, leading to a loss of the composite coating properties. Therefore, fabrication of metal–ceramic composite requires the use of stable suspensions; surfactants are generally used in electroplating solutions to improve the distribution of the particles in the coating [23].

In a previous work [24], Zn–SiC coating electrodeposition was performed by adding industrial additives and 20 g L^{-1} SiC to the same deposition bath studied in the present experimentation. Bright, homogeneous and compact coatings, with low-grain size, were obtained with direct current; however, SiC percentage incorporated in these deposits was found to be very low (<0.1 wt%).

In order to increase the nanoparticle incorporation in the coating, the experimentation was continued by adding different concentrations of gelatine to the bath. On plating with gelatine concentrations lower than 2 g L^{-1}, in absence of nanoparticles, not homogeneous deposits with the presence of flaws on their surface were obtained. Coatings electrodeposited with direct current from the bath with 2 g L^{-1} gelatine were compact and homogeneous, even if the grain size was not low (results not shown in the present work). On depositing in the same experimental conditions, but with 20 g L^{-1} SiC particles in the bath (SiC_b), coatings containing from 1.5 to 2.4 wt% SiC (SiC_d), depending on current density, were obtained. As shown by SEM image reported in Fig. 3a, these deposits have also got a rough surface. In order to improve coating morphology, which is crucial for corrosion resistance, electrodepositions with pulsed direct current (pulse frequency 1 Hz, duty cycle 50 %) were performed in the same bath. Under these experimental conditions, zinc deposits with low-grain size were obtained (Fig. 3b). Visual observation showed that Zn–SiC coatings obtained with direct current appear opaque grey, while those obtained with pulsed current have a shiny and iridescent aspect. Figure 3c shows the EDX map of Si obtained on the deposit in Fig. 3b; the map indicates that SiC particles are equally distributed in the coating. On the basis of these results, the experimentation was continued with 2 g L^{-1} gelatine in the bath and pulsed current.

Figure 4 shows the effect of both temperature and SiC concentration in the bath on particle percentage in the deposits at different average current densities (i_A). SiC content in the coatings increase on increasing current density; this result can be attributed to the strong adsorption promoted by the high overpotential corresponding to increasing current density [6]. Results in Fig. 4 indicate that, on halving SiC bath concentration (curves a and b), only a relatively small decrease in particles percentage in the coating can be obtained at average current densities lower than 100 mA cm^{-2}; this difference gradually decreases on increasing i_A from 100 to 150 mA cm^{-2} and completely disappears at 150 mA cm^{-2}. A limited effect of the increase in SiC concentration in the bath on SiC incorporation rate was found also by Tulio et al. [17] for Zn–Ni–SiC composite electrodeposition. The increase in temperature from 33 to 45 °C (curves a and c, respectively) leads to a significantly decrease in the SiC percentage incorporated in the deposit for i_A values lower than 150 mA cm^{-2}. This decrease can be explained by considering that the increase in temperature favours the electroactive specie reduction, while it does not increase the particle incorporation rate, as suggested by Narasimman et al. [25] for codeposition of Ni and nano SiC. It is noteworthy that the increase of 12 °C in temperature leads to a decrease in SiC wt% in the deposit more marked than that obtained by halving particles concentration in the bath.

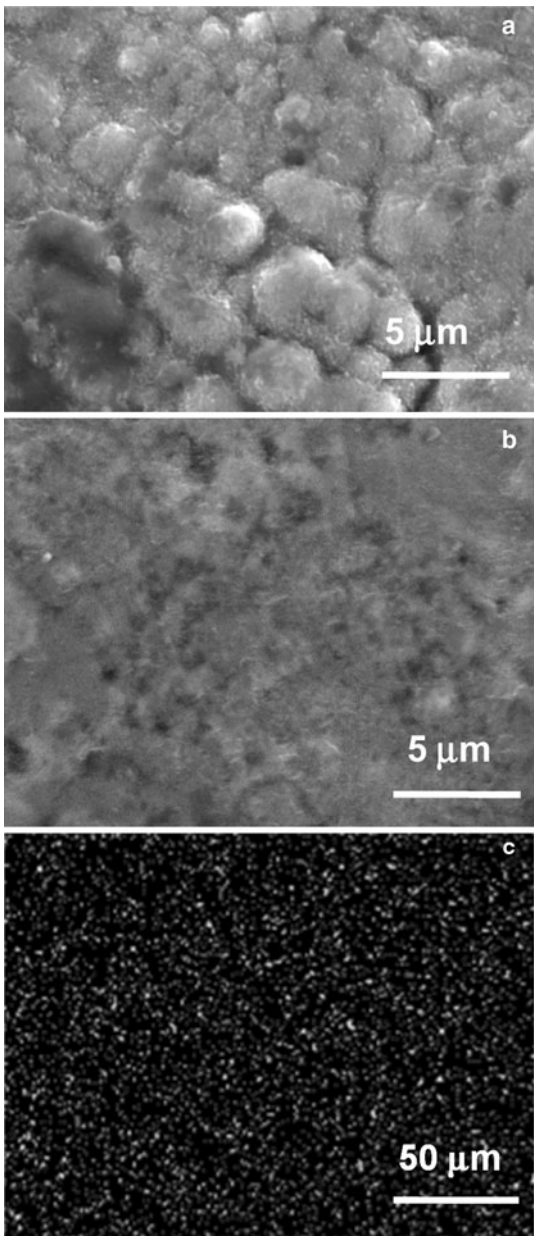

Fig. 3 SEM images of the Zn–SiC coatings obtained at 45 °C from the bath containing 20 g L^{-1} SiC and 2 g L^{-1} gelatine with: **a** direct current density: 150 mA cm^{-2}, SiC_d 2.4 wt%; **b** average pulsed current density (i_A): 150 mA cm^{-2}, SiC_d 2.1 wt%. **c** EDX map of Si (*white colour*) obtained on the coating in (**b**)

The effect of bath temperature and SiC particles concentration on current efficiency at different average current densities is shown in Fig. 5. The curve related to pure zinc deposition, performed at 45 °C from the bath without SiC, is also reported. Pure zinc deposition (curve a) shows very high-current efficiencies, which can be attributed to the presence of gelatine in the bath [26, 27]. The current

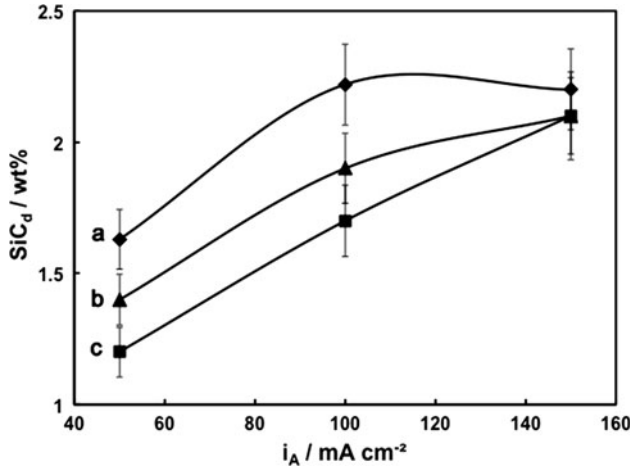

Fig. 4 Effect of bath temperature and SiC content in the bath on SiC content in the deposit at different average current densities: (*a*) SiC_b 20 g L^{-1}, *T* 33 °C; (*b*) SiC_b 10 g L^{-1}, 33 °C; (*c*) SiC_b 20 g L^{-1}, 45 °C

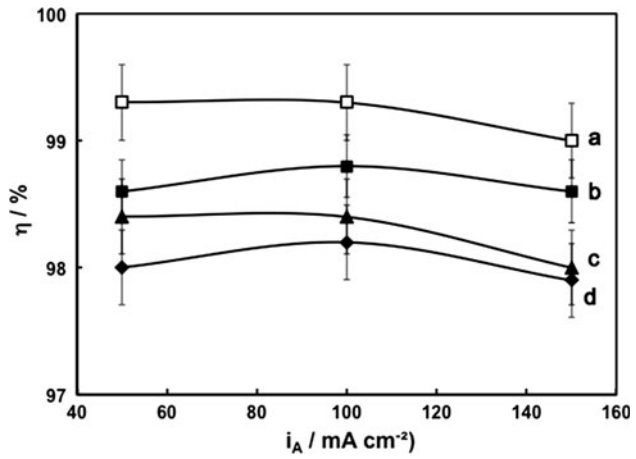

Fig. 5 Effect of bath temperature and SiC content in the bath on current efficiencies at different average current densities (*a*) SiC_b 0 g L^{-1}, *T* 45 °C; (*b*) SiC_b 20 g L^{-1}, 45 °C; (*c*) SiC_b 10 g L^{-1}, 33 °C; and (*d*) SiC_b 20 g L^{-1}, *T* 33 °C

efficiency decreases when 20 g L^{-1} SiC is added to the bath (curve b), which is consistent with other authors results [17]. The decrease in deposition temperature from 45 to 33 °C leads to a further decrease in current efficiency (curve d), while on decreasing SiC_b from 20 to 10 g L^{-1} (curves d and c, respectively) only a small increase in η can be obtained. Results in Fig. 5 indicate that the lowest current efficiencies were obtained in the experimental conditions, which enhance SiC incorporation i.e. at the lower temperature (33 °C) and with the higher SiC concentration in the bath (20 g L^{-1}). However, it is noteworthy that η values are always very high (>97.5 %); this result can be attributed to the fact that the amount of particles incorporated is relatively low.

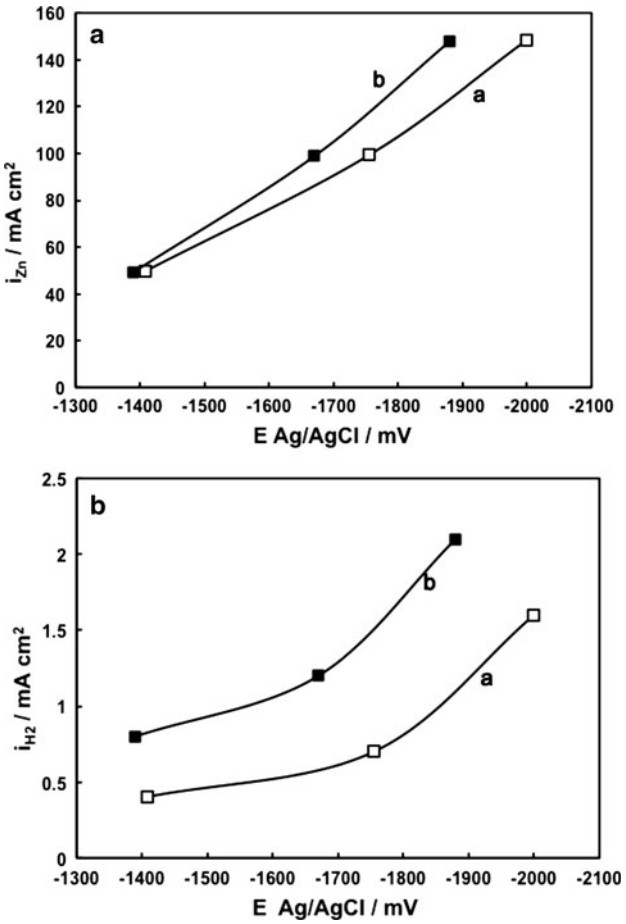

Fig. 6 **a** Zn partial current densities; *curve a*: bath without SiC; *curve b*: bath with 20 g L^{-1} SiC. **b** H_2 partial current densities; *curve a*: bath without SiC; *curve b*: bath with 20 g L^{-1} SiC. *T* 45 °C

Figure 6 shows Zn and H_2 partial current densities related to the elctrodepositions performed at 45 °C with the bath containing 20 g L^{-1} SiC and with the bath without nanoparticles; SiC shifts reduction potential of zinc and hydrogen ions to more positive potentials, with an increase in both partial current densities, in agreement with other authors results [16, 17]. Several hypotheses have been proposed to explain similar effects of the inert particles on cathodic reactions: increase in cathode surface area due to the adsorbed particles [28], change in texture promoted by the particles [29], migration component [28] and turbulent flow promoted by the particles [30]. Tulio and Carlos [16] suggest that SiC may be thought of as additive that promotes Zn electrodeposition from acidic solutions. At the highest potentials, the incorporation of SiC increases H_2 partial current, more than the zinc one, leading to the higher difference between current efficiencies (Fig. 5, curves a and b).

Results reported in Fig. 4 shows that at 45 °C SiC content is lower than that obtained at 33 °C, however, on comparing Fig. 3b with Fig. 7, it can be observed that the

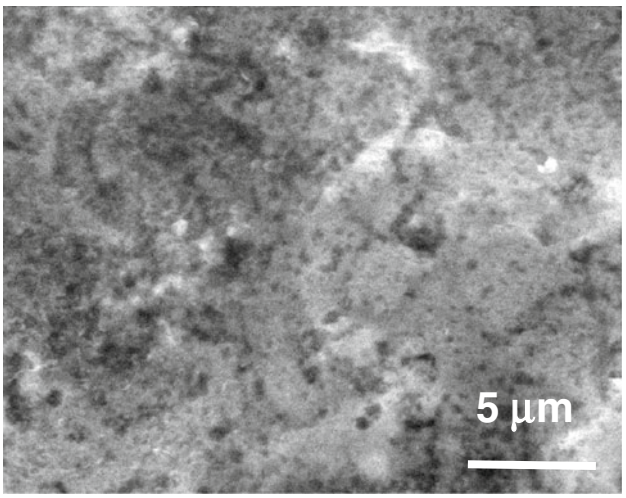

Fig. 7 SEM image of the coating electrodeposited at 33 °C with i_A 150 mA cm^{-2}. SiC_b 20 g L^{-1}. SiC_d 2.2 wt%

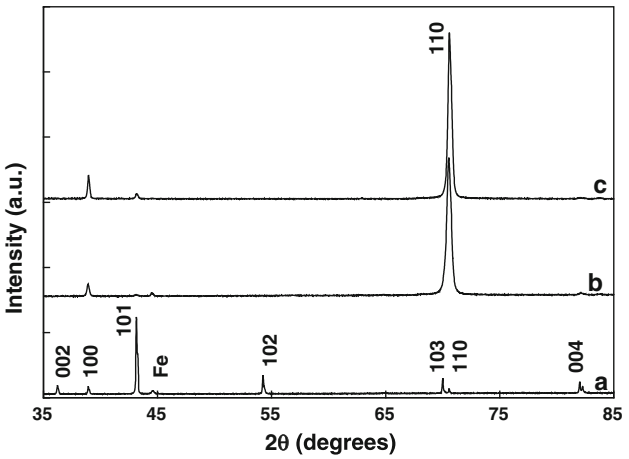

Fig. 8 XRD patterns of zinc coatings electrodeposited from (*a*) bath without additives; (*b*) bath with 2 g L^{-1} gelatine and (*c*) bath with 2 g L^{-1} gelatine and 20 g L^{-1} SiC, i_A 100 mA cm^{-2}, *T* 45 °C

decrease in temperature makes the coating morphology worse, with a visible increase in roughness.

The effect of the addition of gelatine and SiC to the deposition bath on zinc coating structure is shown in Fig. 8. All the deposits are crystalline; the 2θ values of the peaks related to zinc deposit obtained from the bath without gelatine and SiC (pattern a) are in good agreement with the standard values (JCPDS 4-0831), with the predominant (101) reflection. The addition of gelatine to the deposition bath (pattern b) leads to a strong orientation of zinc deposit and the reflection from the (110) plane becomes largely predominant. This result is consistent with what has been found also by other authors for zinc electrodeposited from highly acidic solutions containing gelatine [27]. Xia et al. [31] attributed the effect of gelatine on zinc crystallographic orientation and morphology to its adsorption on the surface of the growing deposit. Mackinnon and Brenner [32] suggested that (110) preferred orientation is related to the higher overpotential induced by the use of organic additives. The incorporation of SiC does not change the zinc structure appreciably (pattern c); the small increase in intensity of all the peaks in the Zn–SiC XRD pattern is due to a slight higher thickness of this coating, as demonstrated by the absence of the Fe main peak. No signal related to the SiC main peak is detectable in this diffractogram, due to the low percentage of particles in the deposit. On changing average current density in the range 80–150 mA cm^{-2}, results quite similar to those reported in Fig. 8 are found.

Figure 9 shows the effect of the addition of gelatine and SiC particles to the bath on zinc coating morphology. Zinc deposit obtained from the bath without additives, (Fig. 9a) shows large hexagonal crystals, typical of pure zinc. The addition of 2 g L^{-1} gelatine to the deposition bath leads to a strong decrease in the zinc grain size (Fig. 9b); similar results was found also by Sekar and Sobha Jayakrishnan [26] for pure zinc electrodeposited from an acetate electrolyte. SiC incorporation does not affect morphology markedly: only a very slight increase in deposit roughness can be observed in Fig. 9c. SEM image of a cross-sectional area of the coating in Fig. 9c, obtained after brittle fracture in liquid N_2, is shown in Fig. 9d; a cubic βSiC particle (about 70 nm in size) partially embedded in the metal matrix is clearly visible in the photo. EDX punctual analysis showed Si signal in other zones of the coating shown in Fig. 9d, indicating the presence of more nanosized particles, but they are hardly visible in the photo because they are almost entirely covered by zinc. EDX map for Si, performed on the whole cross section (Fig. 10a), shows that SiC particles are distributed within the entire coating layer (Fig. 10b).

XRD pattern related to the coating obtained at 50 mA cm^{-2} from the bath with gelatine and without SiC (Fig. 11a, pattern a) indicates that the preferred orientation induced by gelatine at this current density is smaller than that induced at higher current densities (Fig. 8). The incorporation of SiC particles decreases zinc preferential orientation (Fig. 11a, pattern b). SEM image of the coating with nanoparticles electrodeposited at 50 mA cm^{-2} (Fig. 11b), show the formation of large hexagonal grains aligned vertically in different directions; the same morphology, but with a slightly lower grain size, was observed on the deposit obtained at the same current density without nanoparticles. A similar morphology has been observed also by Baik and Fray [27] for pure zinc electrodeposits obtained from chloride bath containing gelatine.

Figure 12 reports the results of microhardness measurements, performed on the coatings elecrodeposited from

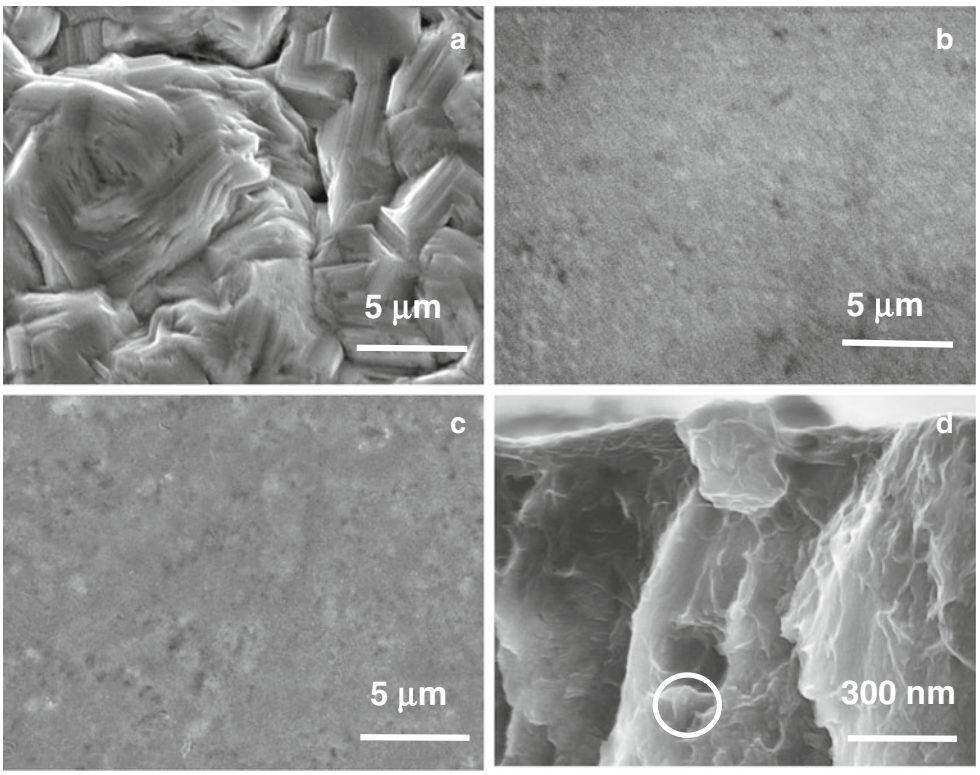

Fig. 9 SEM images of zinc coatings electrodeposited at 45 °C and i_A 100 mA cm^{-2} from: **a** bath without additives; **b** bath containing gelatine 2 g L^{-1}; **c** bath containing gelatine 2 g L^{-1} and SiC 20 g L^{-1}, SiC_d 1.7 wt%. **d** SEM image of a cross sectional area of the coating in photo c, after brittle fracture in liquid N_2

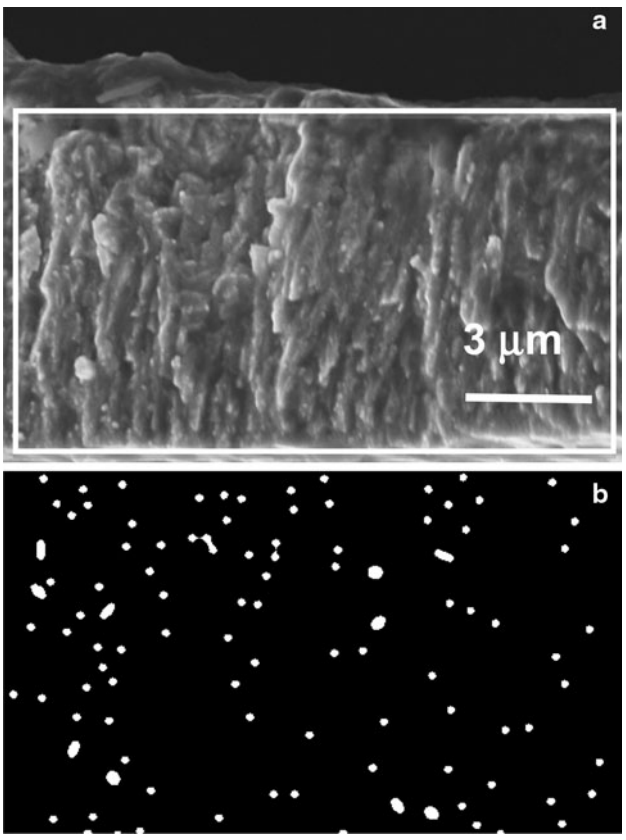

Fig. 10 **a** SEM image of the whole cross section of the coating in Fig. 9c. **b** EDX map for Si (*white colour*) carried out on the area marked with *white rectangle* in (**a**)

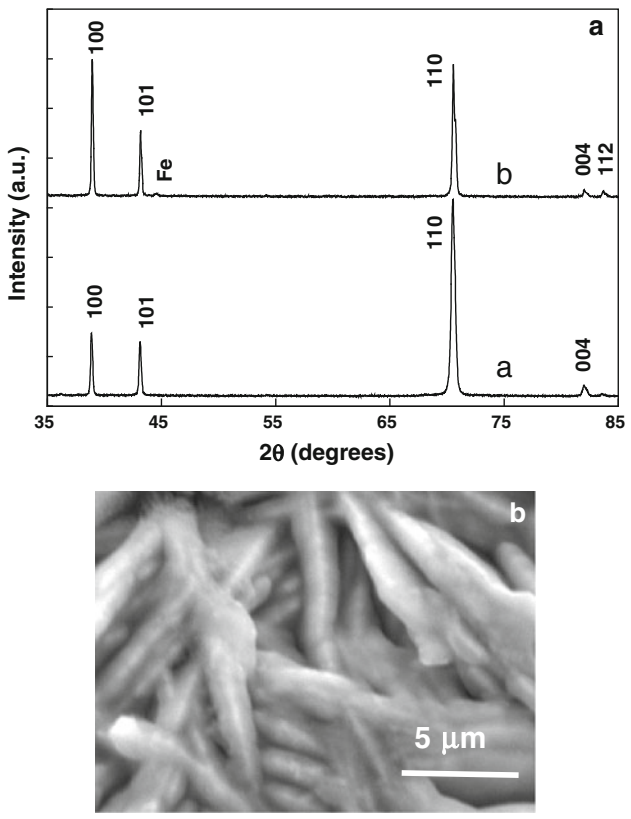

Fig. 11 **a** XRD patterns of zinc coatings electrodeposited from the baths containing 2 g L^{-1} gelatine (pattern a); 2 g L^{-1} gelatine and 20 g L^{-1} SiC (pattern b). **b** SEM image of the deposit obtained from the bath containing 2 g L^{-1} gelatine and 20 g L^{-1} SiC (SiC_d 1.2 wt%). i_A 50 mA cm^{-2}. T 45 °C

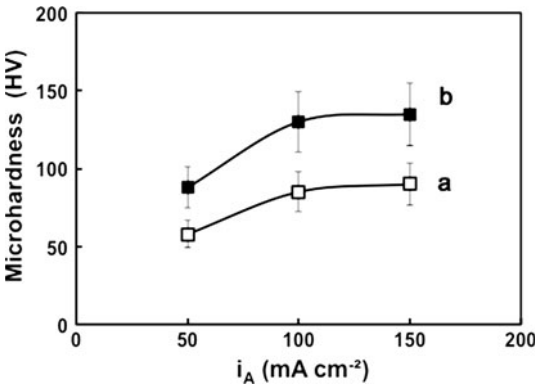

Fig. 12 Vickers microhardness of the coatings electrodeposited at 45 °C from: (*a*) bath without SiC particles; (*b*) bath containing 20 g L^{-1} SiC

baths with and without SiC particles. Microhardness of both deposits increase with an increase in average current density from 50 to 100 mA cm^{-2} while only a small difference was found between 100 and 150 mA cm^{-2}. These results can be related to the strong decrease in deposit grain size obtained by increasing current density from 50 mA cm^{-2} (Fig. 11b) to 100 mA cm^{-2} (Fig. 9c). The incorporation of SiC nanoparticles leads to an increase in microhardness of about 50 % at all the average current densities studied.

4 Conclusions

Zn–SiC composite coatings have been successfully obtained by electrodeposition on mild steel substrate. A slightly acidic chloride bath containing gelatine and SiC nanoparticles (average crystallite size: 60 nm) was used. The electrodepositions were performed under galvanostatic control with pulsed direct current density. From the results, the following conclusions can be drawn:

(1) Coatings electrodeposited with pulsed current have better morphology than those of the deposits obtained with direct current, with the grain size markedly smaller.
(2) The increase in temperature from 33 to 45 °C leads to a significantly decrease in the SiC percentage incorporated in the deposit, but improves the coating morphology.
(3) On halving SiC concentration in the bath, only a small decrease in deposit SiC content is obtained.
(4) In all the experimental conditions of the present research, current efficiencies are higher than 97.5 %.
(5) At 45° C, with 20 g L^{-1} SiC in the bath and average current density in the range 100–150 mA cm^{-2}, homogeneous and compact coatings, with small grain size and SiC content in the range 1.7–2.1 wt% were obtained.
(6) Microhardness measurements show for these deposits an increase of about 50 % with respect to those obtained without nanoparticles in the same experimental conditions.

Acknowledgments The authors thank Dr M. Lekka and Prof. L Fedrizzi for their useful suggestions.

References

1. Musiani M (2000) Electrochim Acta 45:3397
2. Low CTJ, Wills RGA, Walsh FC (2006) Surf Coat Technol 201:371
3. Wu G, Li N, Zhou D, Mitsuo (2004) Surf Coat Technol 176:157
4. Shrestha NK, Sakurada K, Masuko M, Saji T (2001) Surf Coat Technol 140:175
5. Aslanidis D, Fransaer J, Celis JP (1997) J Electrochem Soc 144:2352
6. Gomes A, Pereira I, Fernández B, Pereiro R (2011) In: Boreddy Reddy (ed) Advances in Nanocomposites—Synthesis, Characterization and Industrial Applications, InTech, p 503
7. Roos JR, Celis JP, Fransaer J, Buelens C (1990) JOM 42:60
8. Celis JP, Roos JR, Buelens C, Fransaer J (1991) Trans Inst Metal Finish 69:133
9. Hovestad A, Jansen LJJ (1995) J Appl Electrochem 25:519
10. Guglielmi N (1972) J Electrochem Soc 119:1009
11. Frade T, Bouzon V, Gomes A, da Silva Pereira MI (2010) Surf Coat Technol 204:3592
12. Zhou YB, Qian BY, Zhang HJ (2009) Thin Solid Films 517:3287
13. Vlasa A, Varvara S, Pop A, Bulea C, Muresan LM (2010) J Appl Electrochem 40:1519
14. Gyawali G, Cho SH, Woo DJ, Lee SW (2012) Trans Inst Metal Finish 90:274
15. Lekka M, Zanella C, Klorikowska A, Bonora PL (2010) Electrochim Acta 55:7876
16. Tulio PC, Carlos IA (2009) J Appl Electrochem 39:1305
17. Tulio PC, Rodrigues SEB, Carlos IA (2007) Surf Coat Technol 202:91
18. Müller C, Sarret M, Benballa M (2002) Surf Coat Technol 162:49
19. Zheng H, An M, Lu J (2008) Appl Surf Sci 254:1644
20. Vathsala K, Venkatesha TV (2011) Appl Surf Sci 257:8929
21. Kondo K, Ohgishi A, Tanaka Z (2000) J Electrochem Soc 147:2611
22. Brenner A (1963) Electrodeposition of Alloys. Academic Press, New York, London, p 350
23. Bindiya S, Basavanna S, Naik YA (2012) J Mater Eng Perform 21:1879
24. Roventi G, Bellezze T, Fratesi R (2012) Proceedings of IX AIMAT National Congress, Gaeta, 16–19 September, p 459
25. Narasimman P, Pushpavanam M, Periasamy VM (2011) Appl Surf Sci 258:590
26. Sekar R, Jayakrishnan Sobha (2006) J Appl Electrochem 36:591
27. Baik DS, Fray DJ (2001) J Appl Electrochem 31:1141
28. Benea L, Bonora PL, Borello A, Martelli S, Wenger F, Ponthiaux P, Galland J (2001) J Electrochem Soc 148:C461
29. Socha RP, Nowak P, Laajalehto K, Väyrynen J (2004) Colloids Surf A 235:45
30. Lee EC, Choi JW (2001) Surf Coat Technol 148:234
31. Xia X, Zhitomirsky I, McDermid JR (2009) J Mater Process Technol 209:2632
32. Mackinnon DJ, Brannen JM (1977) J Appl Electrochem 7:451